Thermal Degradation of Aliphatic–Aromatic Polyamides: Kinetics of *N,N'*-Dihexylisophthalamide Neat and in Presence of Copper Iodide

LINDA J. BROADBELT,[1,*] MICHAEL T. KLEIN,[1,†] BARRY D. DEAN,[2] and STEPHEN M. ANDREWS[2]

[1]Department of Chemical Engineering, University of Delaware, Newark, Delaware 19716 and [2]Amoco Performance Products, Inc., Alpharetta, Georgia 30202

SYNOPSIS

An experimental study to determine the effect of copper (I) iodide (CuI) on the rate and product distribution of degradation of a model of an aliphatic–aromatic polyamide was carried out. *N,N'*-Dihexylisophthalamide (DHI) was reacted in both an inert argon atmosphere and a pure oxygen environment at 350°C with CuI added in amounts ranging from 0 to 20% by weight. The rate of disappearance of DHI was enhanced by an order of magnitude when 0.5% by weight of CuI was added and was an increasing function of increasing CuI loading. Reaction in pure O_2 increased the rate of DHI degradation by two orders of magnitude over that for neat DHI pyrolysis. The rate of disappearance of DHI in O_2 was relatively unchanged when 5% CuI by weight was added. The transformations of DHI and its products are organized in terms of a set of reaction rules. This "reaction operator" formalism allowed computer generation of the reaction network and facilitated estimation of kinetic parameters. © 1995 John Wiley & Sons, Inc.

INTRODUCTION

The polymers in the polyamide family are used for their combination of elasticity, toughness, and abrasion resistance. Aromatic containing polyamides are used as specialty fibers that have unusual heat resistance and outstanding strength to weight ratios.[1] When exposed to elevated melt processing temperatures and harsh processing environments, thermal degradation reactions occur according to a complex network of parallel and series steps. Increased understanding of this network is a reasonable first step in the development of strategies for minimizing thermal degradation or its deleterious effects.

The study of the thermal degradation of polyamides has traditionally involved reaction of the actual polymers. Results include a measure of stability and the identity of the reaction products evolved upon heating. For example, Krasnov et al.[2] studied the vacuum pyrolysis of the aromatic polyamide synthesized from 1,3-phenylenediamine and isophthalic acid. The results were reported in terms of thermal degradation rates and products formed, and some mechanistic speculation was put forth; homolytic degradation pathways were not considered. However, no kinetic analysis was performed to confirm the proposed pathways. Work performed by Ehlers et al.[3] suggested a combination of bond cleavages leading to free radical intermediates. Chatfield et al.[4] attempted to rectify this mechanistic dispute through careful product analysis using infrared and mass spectrometry. The cleavage of the C—N amide bond and the scission of the aromatic C—N bond were the primary degradation pathways. However, the literal elementary step of direct cleavage of the Ar C—N bond is highly energetically unfavorable[5] and therefore probably not representative of the complete mechanistic scenario. The mechanistic picture was further diversified by Ballistreri et al.[6] who incorporated aliphatic acids of varying chain length, *n*, in polyamides synthesized

* Current address: Department of Chemical Engineering, Northwestern University, Evanston, IL 60208.

† To whom correspondence should be addressed.

Journal of Applied Polymer Science, Vol. 56, 803–815 (1995)
 CCC 0021-8995/95/070803-13

from phenylene diamines to probe the effect of n on the thermal decomposition reactions. The products reported were attributed to the scission of the C—N amide linkage for all n. For $n = 2$, the primary thermal decomposition process was proposed to be an intramolecular transfer of hydrogen from one N—H group to a second. The proposed thermal degradation process for $n = 4$ was a concerted transfer of hydrogen from the fourth methylene group to the amide N—H. However, the lack of quantitative yields prevented assessment of the product selectivities and relative reaction rates of bond cleavages and transfer reactions.

These analyses of polyamide thermal degradation provided insight into product identification and several possible degradation mechanisms. This motivated the current work into the fundamentals underlying polyamide thermal degradation using quantitative model compound kinetic studies. This should allow clearer focus on reaction mechanisms and permit resolution of pathways and rate constants. *N,N*-Dihexyisophthalamide (DHI) was chosen as a model of a polyamide synthesized from an aromatic acid and an aliphatic amine.

The experimental plan was fashioned after considering polyamide processing conditions and strategies. High performance polyamides are stabilized against atmospheric degradation at elevated temperatures with copper salts and inorganic halides.[7-9] The reaction of oxygen with a polyamide results in the formation of peroxides that react with a hydrogen donor (including the original polymer) to form hydroperoxides. It is hypothesized that the hydroperoxides are decomposed by reaction with the copper halide, and hydroxyl radicals are quenched and thereby prevented from participation in the propagation of degradation reactions.[10] However, copper also catalyzes decarboxylation and decarbonylation reactions. This is particularly relevant in the production of polyamides where acid endcaps are used, and hydrolysis of the amide linkage resulting in acid groups occurs readily. The balance achieved between oxidative stabilization and catalytic degradation has not been qualitatively or quantitatively assessed. Collectively, these issues suggested that the present study of the reaction of DHI should include experiments in both an inert argon atmosphere and a pure oxygen environment at 350°C in the presence of copper (I) iodide (CuI).

EXPERIMENTAL

The experimental plan for studying the thermal reactions of DHI in inert and oxidative environments and in the presence of CuI is summarized in Table I.

Reactions of DHI were carried out at 350°C in an inert argon atmosphere and in pure O_2, both with and without added CuI, to simulate polyamide processing environments. Reaction times typically ranged from 5 to 210 min, and CuI loadings varied from 0 to 20% by weight. The batch reactions in an argon atmosphere were carried out in 2-mL glass ampoules (Wheaton). Approximately 40 mg of DHI were placed in the glass ampoule that was purged and flame sealed. This reactor was placed in an isothermal fluidized sand bath for the predetermined reaction time, after which it was removed and cooled at room temperature. The reactions in O_2 were carried out in 14-mL stainless steel batch reactors fitted with a valve. This enabled addition of O_2, via cycle purging to the desired pressure, and the collection of product gases. CuI (Aldrich) was used as received and added to the appropriate reaction vessel to achieve the desired loading.

Product recovery was accomplished by dissolving the reaction products in 1,1,1,3,3,3-hexafluoro-2-propanol (Sigma). Product quantification was by gas chromatography (GC) using an HP5890 Gas Chromatograph equipped with a Flame Ionization Detector and an Ultra 2 5% Crosslinked Phenyl Methyl Silicone capillary column. Biphenyl was added as an external standard. Product identification was by GC/MS (mass spectrometry) using an HP5880 Gas Chromatograph equipped with the same column as described above and a 5970 Series Mass Selective Detector. Material eluting above the quantifiable cutoff of 416 amu was included in a char fraction that also included nonvolatile material.

The foregoing analyses allowed estimation of product yields and selectivities as well as the elutable product recovery index (EPRI), defined as the mass of material recovered in elutable products normal-

Table I Experimental Plan for Reaction of *N,N'*-Dihexylisophthalamide

Weight of DHI	Atmosphere	CuI Loading (wt %)	Time (min)
0.040	Argon	0	0–185
0.040	Argon	0.5	0–190
0.040	Argon	1.0	0–208
0.040	Argon	5.0	0–140
0.040	Argon	20.0	0–120
0.070	O_2 25 psig	0	0–40
0.070	O_2 25 psig	5	0–60

All reactions were carried out at 350°C.

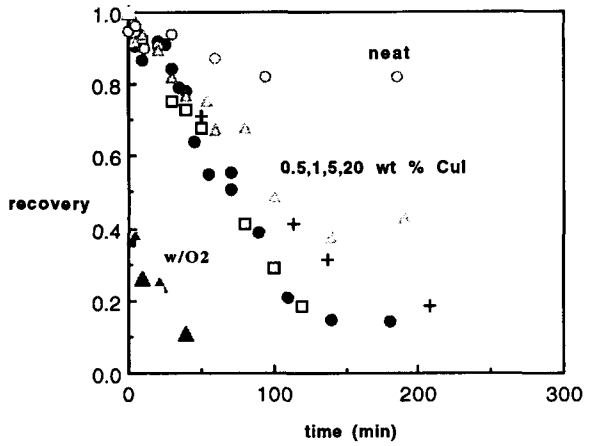

Figure 1 Temporal variations of the disappearance of *N,N'*-dihexylisophthalamide as a function of CuI loading and reaction atmosphere.

ized by the mass of reactant converted. The selectivity to char and light gases was appreciable, as EPRI values ranged from a high of 0.580 when DHI was reacted to a conversion of 0.90 with 20 wt % CuI added to a low of 0.035 when DHI was reacted with an O_2 atmosphere to a conversion of 0.90. In general, EPRI increased with the addition of CuI.

RESULTS

Reactant Recovery

The dramatic influence of CuI and O_2 on the rate of disappearance of DHI is illustrated in Figure 1, the history of the thermal conversion of DHI for each set of reaction conditions studied. Neat pyrolysis was slowest; only about 20% conversion was attained after 200 min at 350°C. Reaction with added O_2 was fastest; approximately 90% conversion was realized after only 40 min. This represents an increase in the rate of disappearance of two orders of magnitude over that for neat pyrolysis. These limiting cases were bracketed by experiments in argon with added CuI, that, roughly, all had the same kinetics. Viewed on a finer scale, this disappearance rate increased by an order of magnitude over that for neat pyrolysis to a pseudo-first-order rate constant $k = 0.0052$ min^{-1} for CuI added at 0.5 wt % ($W_{CuI} = 0.5\%$), and was thereafter an increasing function of CuI loading, achieving an asymptotic value of 0.014 min^{-1} for $W_{CuI} \geq 5\%$. Note that the addition of 5% CuI to the reaction mixture did not change the kinetics in an O_2 environment. This suggests that the effects of CuI and O_2 on DHI degradation were nonlinearly additive, and the catalytic degradation due to CuI was counterbalanced by an increase in oxidative stability due to the presence of CuI. The foregoing patterns in the DHI disappearance kinetics are captured in terms of the pseudo-first-order rate constants reported in Table II.

General Product Spectrum

Representative product selectivities are summarized in Table III for typical reaction conditions. Under all reaction conditions the major products were *m*-cyano-*N*-hexylbenzamide (*m*CNHB); *N,N,N'*-trihexylisophthalamide (THI); *N*-hexylbenzamide (NHB); *N*-hexylisophthalamide (NHI); dihexylamine (DHA); and a collection of hexenes that was predominantly 1-hexene.

Formation of these major products can be viewed in terms of the fragmentation of individual moieties in DHI as illustrated in Figure 2. The cleavage of the amide nitrogen — methylene carbon bond leads to the formation of *m*CNHB (R1) or NHI (R4) and the corresponding hexene. *m*CNHB was the product formed in the highest yield and with the highest selectivity. NHB represents either the cleavage of the amide carbon — nitrogen bond (R3), and subsequent decarbonylation, or the direct cleavage of the aryl carbon — carbonyl carbon bond with hexylamine (HAM) as the resultant coproduct. Hexene is evidently consumed via addition reactions; addition to DHI yields THI (R2) and addition to HAM results in DHA. THI was formed with the second highest selectivity.

The initial slopes in the time history profiles of DHI reaction products reveal important information about the primary or secondary nature of the products. The initial slope of the temporal yield curve for *m*CNHB implicated it clearly as a primary prod-

Table II Increase in Pseudo-First-Order Rate Constants for Reaction of DHI with Increasing CuI Loading in Inert and Oxidative Environments

No.	Atmosphere	CuI Loading (wt %)	k_{1st} (min^{-1}) × 10^2
1	Argon	0	0.096
2	Argon	0.5	0.52
3	Argon	1.0	0.83
4	Argon	5.0	1.40
5	Argon	20.0	1.40
6	O_2	0	19.8
7	O_2	5	17.4

Table III Representative Molar Product Selectivities for the Reaction of DHI Neat, with O_2, with an O_2/CuI Mixture, and with CuI at 350°C

		Product Rank	Neat			P_{O_2} = 25 psig	
			11	60	185	10	40
N,N'-Dihexylisophthalamide recovery	C6NCOPhCONC6	0	0.899	0.873	0.818	0.261	0.111
m-Cyano,*N*-hexylbenzamide (*m*CNHB)	NCPhCONC6	1	0.086	0.250	0.327	0.078	0.031
N-Hexylbenzamide (NHB)	PhCONC6	1	0.0	0.026	0.018	0.0	0.0
N,N,N'-Trihexylisophthalamide (THI)	(C6)2NCOPhCONC6	1	0.0	0.082	0.101	0.0	0.0
N-Hexylisophthalamide (NHI)	C6NCOPhCONH2	1	0.0	0.021	0.030	0.045	0.036
Hexene(s) (HXEN)	C6H12	1	0.0	0.0	0.022	0.0	0.0
Dihexylamine (DHA)	C6NC6	2	0.0	0.028	0.020	0.0	0.0
Dicarbonitrilebenzene (DCNB)	NCPhCN	2					
Benzonitrile (BZN)	PhCN	2					
m-Cyanobenzamide (*m*CBZA)	NCPhCONH2	2					
m-Cyano,*N,N*-dihexylbenzamide (*m*CDHB)	NCPhCON(C6)2	2					
Benzamide (BZA)	PhCONH2	2					
N,N-Dihexylbenzamide (DHB)	PhCON(C6)2	2					
N-Methyl-*N*-hexylaniline (MHAN)	PhN(C1)(C6)	3					
N-Methyl-*N*-undecylaniline (MUAN)	PhN(C1)(C11)	3					
N,N-Dihexylaniline (DHAN)	PhN(C6)2	3					
N-Hexylaniline (HAN)	PhNC6	2					

Product rank defines the relationship in the reaction network to the reactant. Numbers in column headings are time in minutes.

uct. The data were less convincing for NHB and NHI, which, however, will also be assumed to be primary because of the presence of two ring substituents, one of which being the unreacted CONC6. Evidently the yields of these products were initially below the analytical detection limits. The clear initial slope of zero in the time history curve for THI indicates it to be a secondary product. The formation of THI from the addition of the primary product hexene to DHI is consistent with this behavior.

The reaction of DHI in the presence of O_2 was quite rapid and yielded only *m*CNHB and NHI as major products. Relative to that for neat pyrolysis, the selectivity to *m*CNHB decreased and the selectivity to NHI increased. The char yield increased drastically, reflected by the decrease in the EPRI from 0.28 to 0.035.

Reaction in the presence of both O_2 and 5 wt % CuI led in general to *m*CNHB with increased selectivity as compared to that from reaction in O_2 alone. The selectivity to NHI decreased slightly. The addition of CuI had a dramatic effect on the kinetics of NHB formation. NHB did not form upon reaction of DHI with O_2 alone, but the selectivity to NHB in the presence of CuI was 0.176 after 60 min. This is also greater than the value of 0.026 for neat DHI pyrolysis. Benzonitrile was also detected as a product when CuI was present.

The reaction environment affected the DHI product spectrum at low and high conversions alike. At low conversions, the EPRI and the yields and selectivities for the four major aromatic products all increased at the expense of char as W_{CuI} increased. The selectivity to NHB was a very strong function of the added CuI. For W_{CuI} = 0.5%, the selectivity to NHB increased from the neat value of 0.02 to 0.16 at a constant DHI conversion of 0.15. This was a selectivity enhancement ($[y/x]_{CuI}/[y/x]_{neat}$) of 8. As W_{CuI} increased to 5 wt %, the selectivity to NHB increased to approximately 0.32 at the same conversion level. The enhancement in the selectivities to NHI and *m*CNHB were 2.3 and 0.7, respectively, at 0.15 conversion of DHI. The kinetics of *m*CNHB and NHI formation indicate that the rate of cleavage of the N—C bond was accelerated. The selectivity to THI increased with the addition of 0.5 wt % CuI as compared to neat pyrolysis, then decreased as the CuI was increased to 20 wt %.

Overall, the selectivity to NHB was an increasing, nonlinear function of CuI loading at a given conversion. This suggested an increase in the rate of scission of the amide C—N bond, followed by rapid decarbonylation, or a CuI-mediated scission of the aryl—C bond. This is analogous to the copper salt-mediated decarboxylation of aromatic acids that has been reported by Cairncross and coworkers[11] sug-

Table III (*Continued*)

CuI at 350°C													
P_{O_2} = 25 psig, 5% CuI		0.5% CuI			1% CuI			5% CuI			20% CuI		
10	60	10	54	190	10	50	208	10	55	140	10	50	120
0.353	0.119	0.938	0.754	0.428	0.922	0.711	0.184	0.867	0.552	0.148	0.920	0.677	0.183
0.049	0.038	0.186	0.276	0.288	0.0	0.275	0.196	0.138	0.329	0.202	0.217	0.308	0.189
0.058	0.176	0.104	0.204	0.076	0.0	0.213	0.133	0.118	0.209	0.128	0.182	0.211	0.097
0.0	0.0	0.090	0.136	0.050	0.0	0.092	0.013	0.0	0.062	0.004	0.030	0.084	0.005
0.025	0.015	0.043	0.033	0.051	0.0	0.027	0.026	0.027	0.063	0.045	0.033	0.046	0.046
0.0	0.0	0.0	0.032	0.283	0.0	0.027	0.262	0.0	0.088	0.366	0.0	0.049	—
0.0	0.0	0.029	0.022	0.0	0.0	0.014	0.028	0.0	0.010	0.0	0.022	0.011	0.0
		0.0	0.0	0.023	0.0	0.010	0.0	0.0	0.020	0.052	0.0	0.016	0.035
0.0	0.110	0.0	0.039	0.101	0.0	0.045	0.241	0.0	0.0	0.365	0.0	0.0	0.205
		0	0.0	0.0	0.0	0.0	0.022	0.0	0.013	0.034	0.0	0.0	0.023
		0	0.009	0.011	0.0	0.005	0.007	0.0	0.009	0.003	0.0	0.007	0.003
0.0	0.047	0.044	0.100	0.038	0.0	0.091	0.0	0.0	0.092	0.049	0.0	0.093	0.003
		0.0	0.0	0.005	0.0	0.0	0.004	0.0	0.006	0.002	0.0	0.004	0.001
		0	0.007	0.006	0.0	0.012	0.040	0.0	0.039	0.0	0.0	0.027	—
			0.0	0.0	0.0	0.0	0.0	0.0	0.0	0.004	0.0	0.0	0.003
		0	0.0	0.0	0.0	0.0	0.011	0.0	0.008	0.025	0.0	0.008	0.022
		0	0.0	0.0	0.0	0.0	0.0	0.0	0.0	0.008	0.0	0.0	0.006

gested by the detection and isolation of aryl-copper salts.

The time history of the yield of NHB and THI, two of the major DHI products from reaction in argon with CuI, is summarized in Figure 3. The yields for NHB and THI exhibited distinct maxima in reaction time. Moreover, the maximum for a given species shifted to lower reaction times as W_{CuI} in-

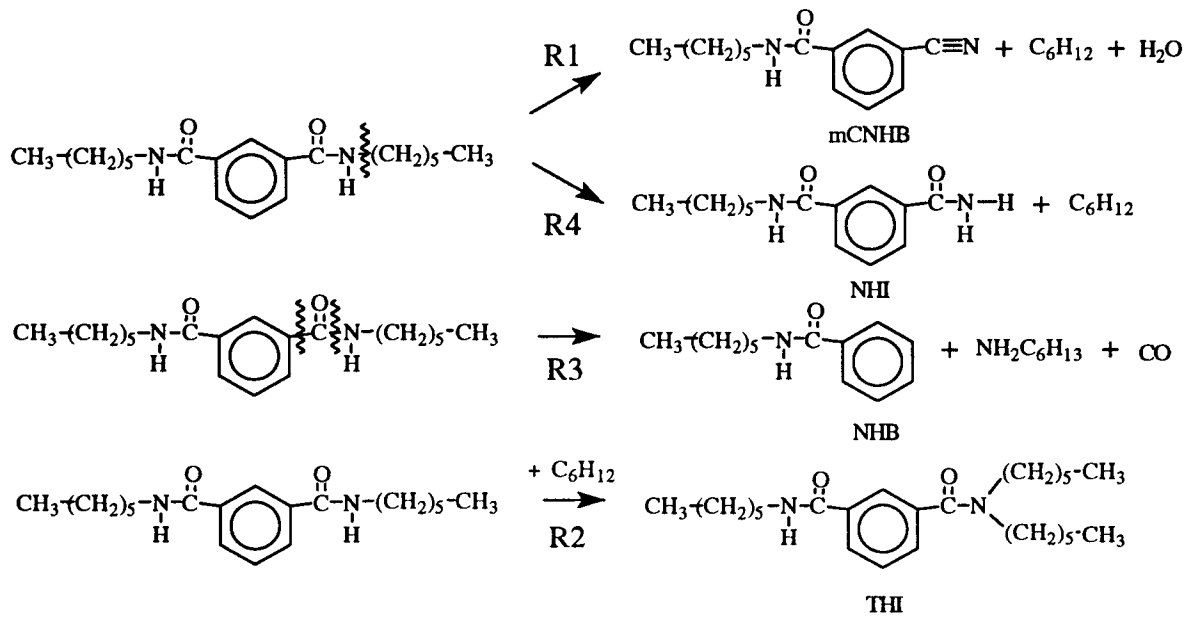

Figure 2 Proposed set of bond cleavages and addition reactions leading to first generation of products.

creased. Qualitatively, these observed shifts can be explained by the increased rate of disappearance of the reactant via all primary pathways, resulting in decreasing rates of formation of primary products.

The kinetics associated with reaction of DHI in the presence of CuI were fast enough to reveal the nonprimary products that evolved from the same set of major, or first generation, products detected from neat pyrolysis. These secondary products included 1,3-dicarbonitrilebenzene, benzonitrile, 3-cyanobenzamide, 3-cyano-*N,N*-dihexylbenzamide, benzamide, and *N,N*-dihexylbenzamide. Figure 4 shows that the same set of bond cleavages and addition reactions that described the DHI reaction paths also lead to the second generation of products when applied to DHI primary products. Thus, the cleavage of the nitrogen — methylene carbon bond affords 1,3-dicarbonitrilebenzene (R1) or *m*-cyanobenzamide (R4) from *m*CNHB, benzonitrile (R1) and benzamide (R4) from NHB, and *m*-cyano-*N,N*-dihexylbenzamide (R1) from THI. Scission of the amide C — N (R3) bond leads to benzonitrile from *m*CNHB, benzamide from NHI, and *N,N*-dihexylbenzamide from THI. The addition of hexene to primary products (R2) results in *m*-cyano-*N,N*-dihexylbenzamide from *m*CNHB and *N,N*-dihexylbenzamide from NHB.

The primary amide functional group of NHI can undergo dehydration to a nitrile. This is analogous to the formation of *m*CNHB from DHI but does not require initial chain cleavage. It is clear from earlier work[5] on substituted benzamides that the dehydration of a primary amide is an order of magnitude faster than that of a secondary amide. Therefore, it seems reasonable to impose some additional chemical significance and segregate the formation of nitriles from amides according to the primary or secondary nature of the reactant.

The dependence of primary and secondary product selectivities on CuI loading can be interpreted in terms of the initial structure of DHI and its primary reactions. The symmetric CONC6 functionality in the original reactant affords primary products that have one of the same functionality intact. The quite reasonable assumption that CuI enhances the rate of reaction of CONC6 as a functional group would suggest further that it enhances the rate of disappearance of the primary products. This in turn affects secondary product selectivities. The data are consistent with this qualitative picture of the CONC6 functional

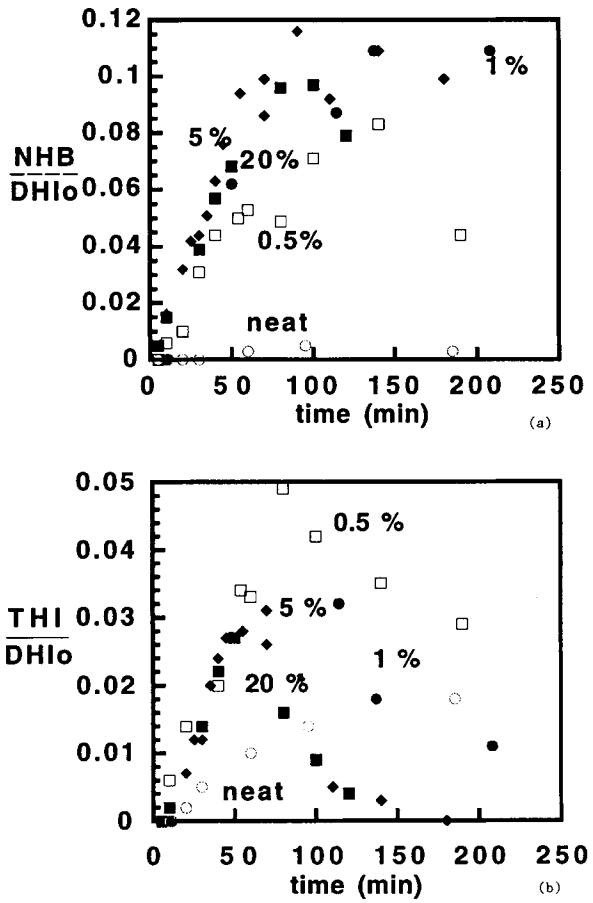

Figure 3 Shift in maximum yield of (a) NHB and (b) THI with increased CuI loading: (○) neat; (□) 0.5%; (●) 1%; (♦) 5%; (■) 20%.

group as a reactive moiety that has a reactivity dependent on the addition of CuI.

This organization of the reaction of DHI and its products allows quantitative kinetic analysis, the first step of which being the deduction of the reaction network or hierarchy of products. As suggested, the primary, or first generation, products from DHI were all accounted for by the application of a small set of bond cleavages and addition reactions. Moreover, the application of this set of transformations to the primary products possessing the appropriate reactive moiety delineated a second generation of species, most of which were quantified experimentally. It thus seems reasonable that a network describing the reaction of DHI and its products can be generated via the successive application of a finite set of reaction rules. It is thus cogent to turn attention to these reaction rules, or operations, that will permit evolution of the reaction network.

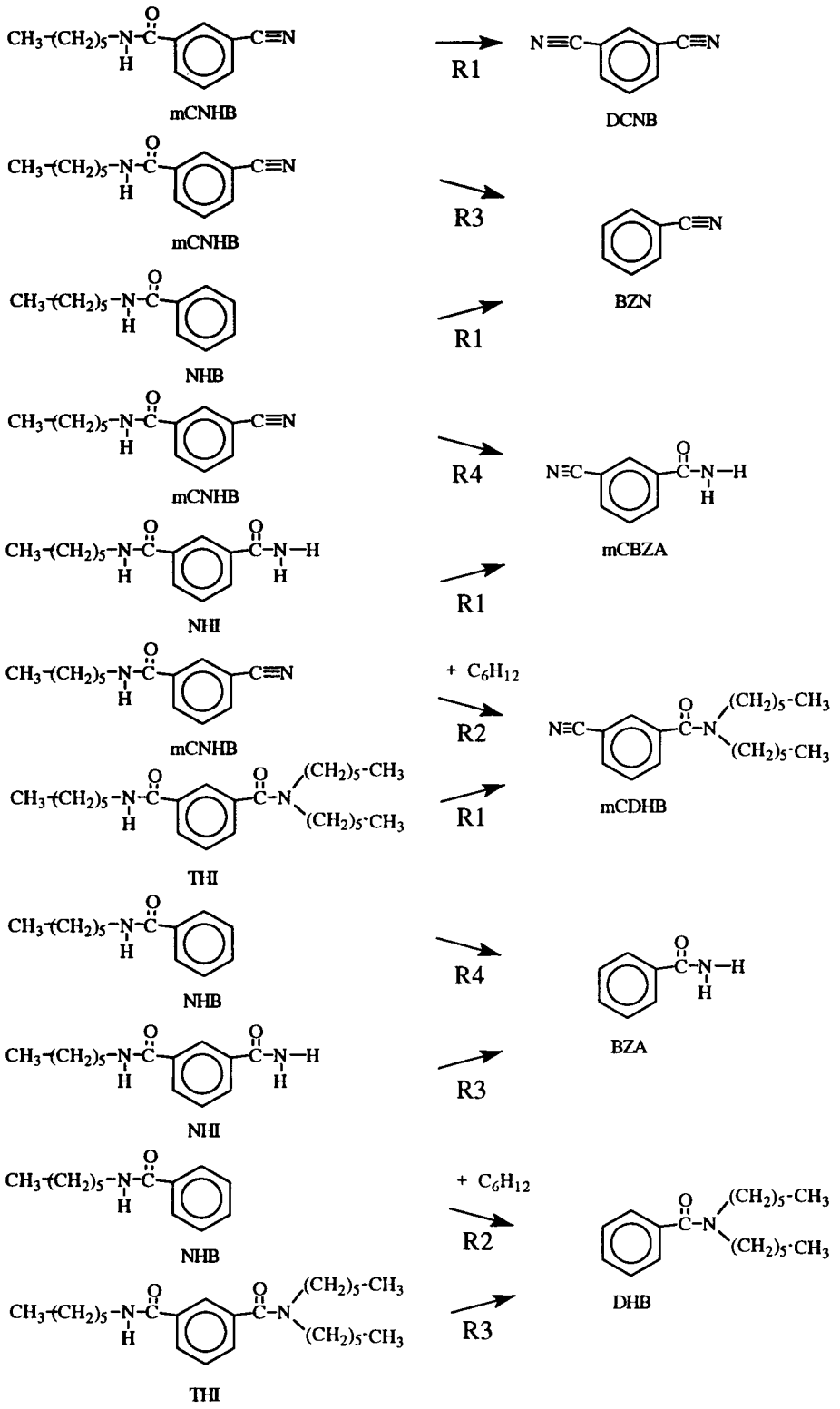

Figure 4 Formation of secondary products from first generation products: application of bond cleavages and addition reactions describing DHI reactivity.

PRODUCT RELATIONSHIPS

As developed in Figures 2 and 4, the major aromatic products and the accompanying light aliphatic products can be generated through the application of five chemical operations to the reactant and subsequent products. The operations effect the following transformations:

Rule 1. a) Formation of a nitrile from a secondary amide; b) formation of a nitrile from a primary amide.

Rule 2. Conversion of a singly substituted hexyl amide to a disubstituted dihexyl amide.

Rule 3. Loss of CONC6.

Rule 4. Formation of a primary amide from a secondary amide.

Rule 5. Loss of CO from a secondary or tertiary amide to yield an aniline derivative.

These operations are illustrated in Figure 5, which depicts the formation of the first generation (primary) products from the parent DHI. Application of these rules to DHI generates the six major products detected from neat DHI pyrolysis. The relative product selectivities of Table III indicate that rules 1 and 3 are the dominant ones. Application of rules 2 and 4 to DHI results in NHB and NHI, whose yields are an order of magnitude lower. Primary amides are generated as products in accordance with rule 4.

The value of these rules is best illustrated through inspection of the high conversion product spectrum resulting from the reaction of DHI in the presence of CuI. This yielded the second tier of products listed in Table III. These products can be generated by the application of the five chemical operators (R1–R5) to the set of DHI primary reaction products.

Exhaustive application of these rules to the reactant and, successively, to each generation of products, created the reaction network. This approach to reaction network generation can be viewed from a purely mathematical perspective: an operator is allowed to act on a function (the reactant) to generate a new function (product) on which the operators can be brought to bear. Clearly, however, optimal network analysis involves the combination of chemical insight and mathematics.

This combination of mathematics and chemistry has some logical consequences. A given product can be obtained from two parents if the same two rules are applied in opposite order. Thus, the chemical operations are commutative with respect to difunc-

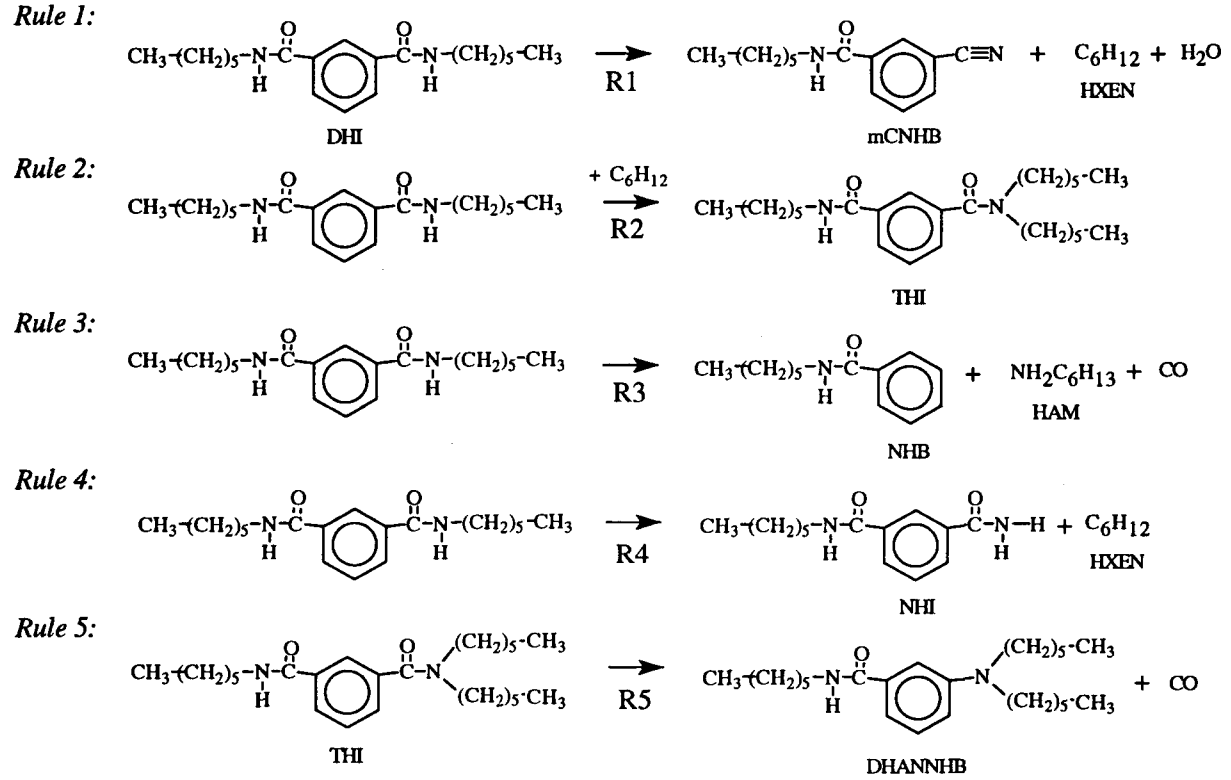

Figure 5 Five chemical operations describing reactions of DHI.

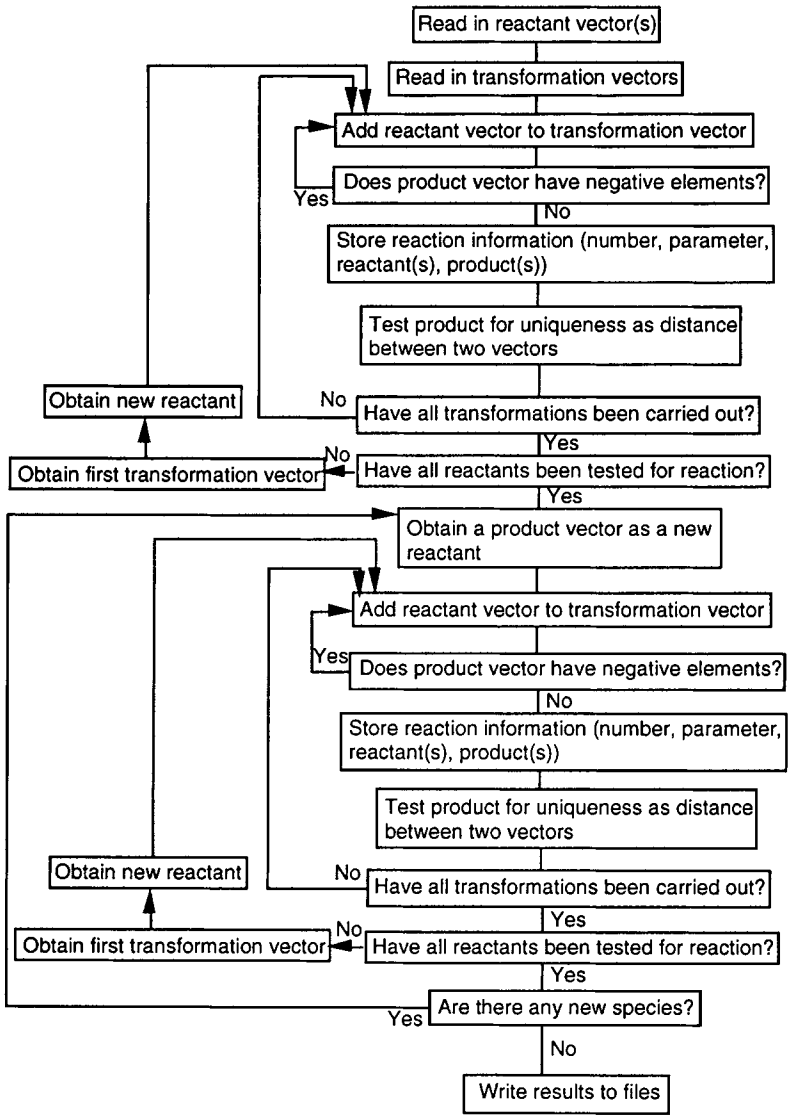

Figure 6 Algorithm for computer generation of the reaction network.

tional species. Provided the appropriate reactive moiety is present, the rules can be applied to the secondary products to form tertiary products, and so on. The evolution of the reaction network is thus explosive; for example, the reactant yields five first-rank products, each of these primary products yields five second-rank products, and so on. In principle, there is a maximum of $\sum_{i=0}^{\infty} 5^i$ species in the reaction network. However, the commutative property of these reaction operators, that is, the nonunique products engendered by application of two rules in a different order, and the formation of unreactive chemical moieties bounds the total number of species. For example, the reaction pathway DHI → *m*CNHB → DCNB results rather quickly in a species that is inert to the chemical operators.

COMPUTER GENERATION OF REACTION NETWORK

The reaction network was generated using the algorithm outlined in Figure 6. The reactants are provided as input in the form of a unique column vector whose rows represented a given aromatic substituent. The numerical value in the row denoted the number of that substituent present. The products that were formed as the reaction network was generated were also designated as

column vectors and thus could be easily subjected to their own reactions. The universally allowed functional groups and a specific example providing the numerical values in each row for DHI are illustrated in Figure 7. More comprehensively, the column vector representation for each of the species detected from reaction of DHI is presented in Table IV.

Each of the reaction rules of Figure 4 was also phrased in terms of a column vector and provided as input to the algorithm. The entries of the vector denoted the disappearance and formation of different functional groups. This is illustrated in Figure 8, which comprises a column vector for each of the reaction rules of Figure 5. For example, the transformation of a CONC6 moiety to a nitrile group, as specified by the chemistry of rule 1, was vectorally designated as $[-1 \quad 0 \quad 1 \quad 0 \quad 0 \quad 0]^T$. The reaction operator is the addition of the reactant vector and the transformation vector.

These vectors are the tools for carrying out reactions. A reaction is engendered when a reaction vector adds to a reactant vector. This is illustrated in Figure 9, where the addition of the vector representing DHI and the vector representing the transformation of an amide group to a nitrile group results in the vector representing *m*CNHB. The product of the reaction is uniquely represented by the column vector that results from this addition. A reactant that could not undergo a given transformation is revealed when an element of the product species vector that would result from the vector addition operation is negative.

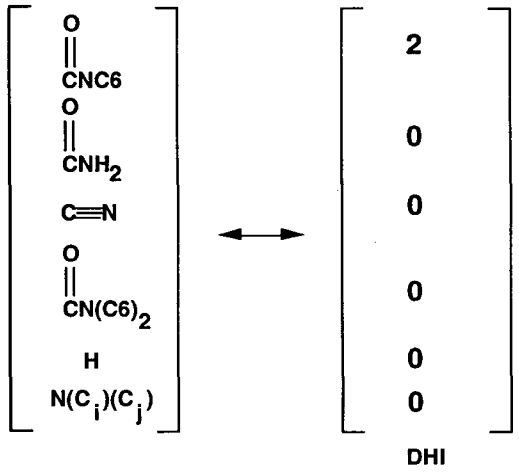

Figure 7 Vector representation of functional groups for DHI and its progeny.

Table IV Column Vector Representation for DHI and Its Progeny

Species	Transpose (T) of Species Column Vector
C6NCOPhNCOC6	[2 0 0 0 0 0]
NCPhCONC6	[1 0 1 0 0 0]
PhCONC6	[1 0 0 0 1 0]
(C6)2NCOPhCONC6	[1 0 0 1 0 0]
C6NCOPhCONH2	[1 1 0 0 0 0]
NCPhCN	[0 0 2 0 0 0]
PhCN	[0 0 1 0 1 0]
NCPhCONH2	[0 1 1 0 0 0]
NCPhCON(C6)2	[0 0 1 1 0 0]
C6H6	[0 0 0 0 2 0]
PhCONH2	[0 1 0 0 1 0]
PhCON(C6)2	[0 0 0 1 1 0]
PhN(C1)(C6)	[0 0 0 0 1 1]
PhN(C1)(C11)	[0 0 0 0 1 1]
PhN(C6)2	[0 0 0 0 1 1]
PhNC6	[0 0 0 0 1 1]

Information is stored for each reaction that includes the rate constant parameter, a unique reaction number, and identities of reactants and products. With this unique vector representation, each of the species can be associated with the reactions that consume it and reactions that generate it. This allows the generation of the differential equations describing the kinetics of the reaction network. The species that are generated as products are tested for species uniqueness. This is accomplished by calculating the distance between the product vector of interest and all of the other previously defined species vectors. If none of the distance values is equal to zero, the species is unique.

The initial portion of the algorithm continues until all of the initial reactants have been subjected to all of the defined chemical transformations. The primary products that were formed as a result of all of the reactants' reactions are then tested for reaction. The algorithm ceases when there are no unreacted unique species.

The output file contains three sets of information. The first is a listing of each of the species in terms of its unique number and the column vector that defines it. Each reaction is written in terms of its unique number, its rate constant, and the reactants involved. All of this information is assembled into a set of differential equations where the dy_i/dt vari-

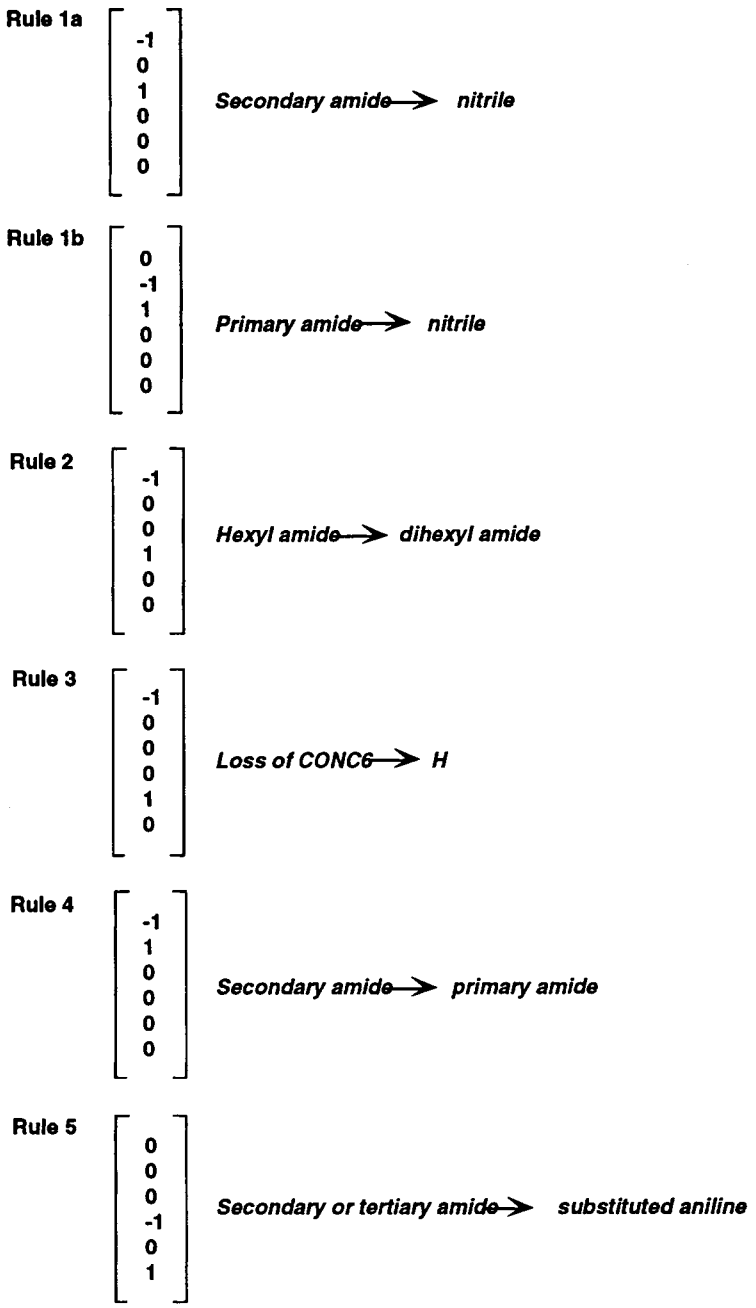

Figure 8 Reaction rule column vectors as expressions of functional group transformations.

able for species i is written as a sum of unique reactions with the appropriate sign to denote species i as a reactant or a product. These equations are exactly in the form that the differential equation solver requires.

RULES BASED NETWORK ANALYSIS

Successive application of the operations to DHI and its progeny generated all of the observed products. The first-pass subsequent kinetics analysis assigned a single rate constant to each of the chemical operations, independent of the reactant that possessed the relevant reactive moiety. The parameters for rules 1a and 2–5 were estimated via global optimization utilizing a Quasi-Newton algorithm for local minimization. The value of the rate constant for dehydration of a primary amide as specified by rule 1b was constrained to be proportional to the rate constant

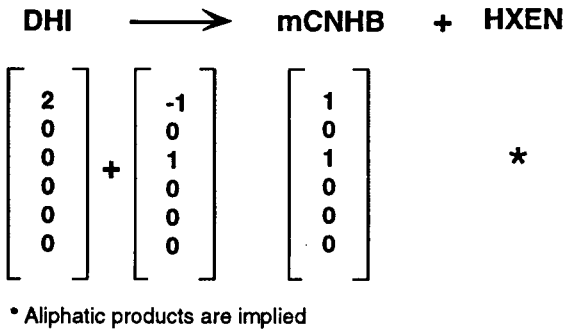

Figure 9 Computer generation of DHI reaction network: reaction is the addition of a reactant vector and a transformation vector.

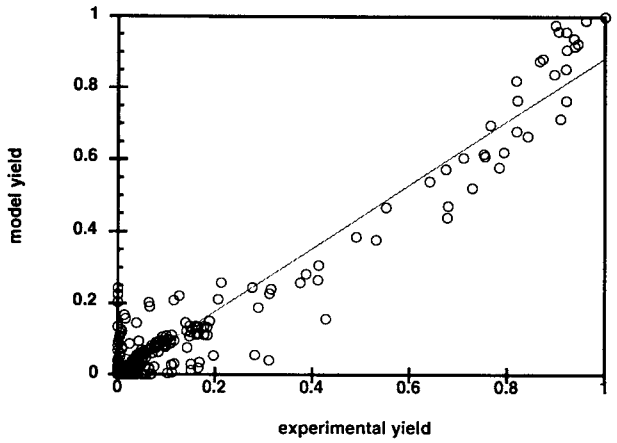

Figure 10 Overall comparison of model predictions and experimental data for reaction of DHI in argon with 0–20 wt % CuI added ($y_P = a + b*y_E$).

for dehydration of a secondary or tertiary amide, for example,

$$k_{1b} = \frac{k_{1a}}{(k_{1a})_{\text{neat}}} * (k_{1b})_{\text{neat}}.$$

The value of $(k_{1b})_{\text{neat}}$ was fixed at the constant value of 0.79 min^{-1} determined from pyrolysis of benzamide.[5] The value of $(k_{1a})_{\text{neat}}$ was determined from optimization of the experimental data for neat pyrolysis of DHI. The results are summarized in Table V.

The accord between model predictions and experimental results is illustrated by the parity plot of Figure 10. The fit of the predicted yields (y_P) to the experimental yields (y_E) was described by the linear equation:

$$y_P = 0.001281 + 0.883 * y_E$$

with a correlation of 0.9698. The most significant deviations of the model predictions from the experimental yields were for hexene and DHI. The experimentally observed sharp increase in hexene yield at long reaction times was predicted at a significantly earlier time. The model also did not predict the dramatic decrease in the disappearance rate of DHI at reaction times greater than 150 min. This suggests the need for additional reactions that account for the formation of DHI from higher rank products. The yield of THI was overpredicted for neat pyrolysis and underpredicted with the addition of CuI. The time predicted for the maximum yield of THI was greater than the experimental value. This was also true for model predictions of the yield of NHB.

The rate constants for rules 1a, 3, and 4 reproduced the trends in the experimental data as a function of CuI loading quite well. The values of k_3 and k_4 increased with increasing CuI loading, contributing to the increased rate of disappearance of DHI and the increased yield of NHB and NHI as CuI increased. The decrease in k_{1a} and the commensurate increase in k_4 with the addition of CuI accounts for the increased yield of *m*CNHB at increased CuI loadings. Although the rate of formation of *m*CNHB directly from the reactant DHI is more rapid than the rate of formation via dehydration of NHI for neat pyrolysis, the relative contribution of these two reaction pathways for *m*CNHB formation is inverted

Table V Network Analysis Rate Constants for Chemical Operations as a Function of Reaction Conditions

k (min^{-1}) $\times 10^4$	1	2	3	4	5
Neat	1.603×10^{-6}	3.197×10^4	0.2961	1.775	94.33
0.5% CuI	2.069×10^{-7}	99.17	6.224	12.16	5.209
1% CuI	1.940×10^{-7}	33.28	9.978	16.51	3.504×10^{-5}
5% CuI	3.671×10^{-7}	44.44	13.21	19.92	8.024×10^{-4}
20% CuI	2.045×10^{-7}	41.08	13.10	24.11	7.279×10^{-7}

T = 350°C, argon atmosphere, 2-mL glass batch reactors.

when CuI is added. The rate constant for the formation of substituted anilines from secondary or tertiary amides (R5) increased with increasing CuI loading at values above 1 wt %. The total yield of substituted anilines was zero for neat pyrolysis and very small for reaction of DHI with 0.5 wt % CuI. The resultant contribution to the objective function was insignificant, and therefore, k_5 was not easily optimized. The application of substituent effects to the rate constant for each reaction rule would be a first step in accounting for differences in reactivity of DHI and its progeny.

CONCLUSIONS

1. The thermal reaction of DHI is through five primary pathways whose rates were variously affected by the presence of O_2 and CuI. The addition of CuI in O_2 and argon led to a dramatic increase in the selectivity to *N*-hexylbenzamide. Secondary products were observed from reaction of DHI with CuI in argon because of faster overall kinetics.
2. Exhaustive application of reaction rules derived from the primary reactions allowed generation of the complete reaction network. The qualitative features of the experiments were captured well. Overall quantitative agreement between model predictions (y_P) and experiments (y_E) was described by the linear equation:

$$y_P = 0.001281 + 0.883 * y_E$$

with a correlation of 0.9698.
3. The effects of the reaction environment were captured in the numerical values of the rate constants. Of particular note, k_1, k_3, and k_4 increased with increasing CuI loading, contributing to the increased rate of disappearance of DHI and the increased yield of *m*CNHB, NHB, and NHI as the loading of CuI increased.

This research was sponsored in part by Amoco Performance Products, Inc. and in part by the State of Delaware as authorized by the State Budget Act of Fiscal Year 1990. The authors would also like to thank Kimberly Fleming and Dave Gayle for their invaluable assistance in the laboratory.

REFERENCES

1. F. W. Billmeyer, *Textbook of Polymer Science,* Wiley, New York, 1984.
2. Y. P. Krasnov, V. I. Logunova, and L. B. Sokolov, *Polymer Science USSR,* **8,** 2176 (1966).
3. G. F. L. Ehlers, K. R. Fisch, and W. R. Powell, *J. Polym. Sci. A-1,* **8,** 3511 (1970).
4. D. A. Chatfield, I. N. Einhorn, R. W. Mickelson, and J. H. Futrell, *J. Polym. Sci., Polym. Chem. Ed.,* **17,** 1353 (1979).
5. L. J. Broadbelt, A. Chu, and M. T. Klein, *Polym. Prepr.,* **34**(2), 235 (1993).
6. A. Ballistreri, D. Garozzo, M. Giuffrida, P. Maravigna, and G. Montaudo, *Macromolecules,* **19,** 2693 (1986).
7. Y. Mahojer, U.S. Pat. 4,745,006 (May 17, 1988).
8. N. Nakamura, Y. Hotta, T. Murakami, Y. Shimpo, K. Etoh, and Y. Shirasaki, U.S. Pat. 3,499,867 (March 10, 1970).
9. G. S. Stamatoff, U.S. Pat. 2,705,227 (March 29, 1955).
10. C. L. Jenkins and J. K. I. Kochi, *J. Org. Chem.,* **36**(21), 309 (1971).
11. A. Cairncross, J. R. Roland, R. M. Henderson, and W. A. Sheppard, *J. Am. Chem. Soc.,* **92**(10), 3187 (1970).

Received July 11, 1994
Accepted November 4, 1994